THE JOURNAL OF BIOLOGICAL CHEMISTRY VOL. 283, NO. 15, pp. 9587–9594, April 11, 2008


# The Nitric Oxide Reductase Activity of Cytochrome *c* Nitrite Reductase from *Escherichia coli*[*]

Received for publication, November 6, 2007, and in revised form, January 11, 2008 Published, JBC Papers in Press, February 1, 2008, DOI 10.1074/jbc.M709090200

**Jessica H. van Wonderen, Bénédicte Burlat[1], David J. Richardson, Myles R. Cheesman, and Julea N. Butt[2]**

*From the Centre for Metalloprotein Spectroscopy and Biology, School of Chemical Sciences and Pharmacy, School of Biological Sciences, University of East Anglia, Norwich NR4 7TJ, United Kingdom*

**Cytochrome *c* nitrite reductase (NrfA) from *Escherichia coli* has a well established role in the respiratory reduction of nitrite to ammonium. More recently the observation that anaerobically grown *E. coli nrf* mutants were more sensitive to NO· than the parent strain led to the proposal that NrfA might also participate in NO· detoxification. Here we describe protein film voltammetry that presents a quantitative description of NrfA NO· reductase activity. NO· reduction is initiated at similar potentials to NrfA-catalyzed reduction of nitrite and hydroxylamine. All three activities are strongly inhibited by cyanide. Together these results suggest a common site for reduction of all three substrates as axial ligands to the lysine-coordinated NrfA heme rather than nonspecific NO· reduction at one of the four His-His coordinated hemes also present in each NrfA subunit. NO· reduction by NrfA is described by a $K_m$ of the order of 300 $\mu$M. The predicted turnover number of ~840 NO· $s^{-1}$ is much higher than that of the dedicated respiratory NO· reductases of denitrification and the flavorubredoxin and flavohemoglobin of *E. coli* that are also proposed to play roles in NO· detoxification. In considering the manner by which anaerobically growing *E. coli* might detoxify exogenously generated NO· encountered during invasion of a human host it appears that the periplasmically located NrfA should be effective in maintaining low NO· levels such that any NO· reaching the cytoplasm is efficiently removed by flavorubredoxin ($K_m$ ~ 0.4 $\mu$M).**

Nitric oxide (nitrogen monoxide or NO·)[3] is functionally important throughout the biosphere (1). In humans it serves as a signaling molecule and vasodilator and in Bacteria and Archaea it can provide a substrate for anaerobic respiration. However, NO· is also a potent cytotoxin that forms part of the innate response of hosts to the infective invasion of pathogens. For this purpose NO· is produced from L-arginine by inducible NO· synthase and from nitrite in response to intragastric acidity (2, 3). As a consequence, enteric food-borne pathogens such as *Escherichia coli* have developed mechanisms for NO· detoxification to ensure their survival in the range of oxic, micro-oxic, and anoxic environments encountered in their animal hosts. *E. coli* lacks genes homologous to those encoding the dedicated respiratory NO· reductases found in bacteria such as *Paracoccus denitrificans* and *Pseudomonas stutzeri* (4, 5). Alternative enzymes must be employed for NO· management, and three in particular have been implicated in the removal of NO·, flavohemoglobin, flavorubredoxin, and cytochrome *c* nitrite reductase (NrfA) (6–8).

Flavohemoglobin is a cytoplasmic protein expressed in the presence of nitrate during aerobic and anaerobic growth (9, 10). In the presence of oxygen flavohemoglobin converts NO· to nitrate at a rate that has been reported to range from 10 to 670 NO· $s^{-1}$. In the absence of oxygen, flavohemoglobin converts NO· to nitroxyl ($NO^-$). However, the rates of NO· reduction are significantly lower than those of NO· oxidation and may not be sufficient for effective NO· detoxification. Under such anoxic conditions flavorubredoxin and NrfA could provide alternative catalysts for NO· removal (6, 11, 12). Flavorubredoxin is a cytoplasmic protein that reduces ~15 NO· $s^{-1}$ with a Michaelis constant ($K_m$) of ~0.4 $\mu$M. However, there is relatively little kinetic information available regarding NO· removal by the periplasmically located NrfA that may represent the first line of defense toward exogenously generated NO·.

A possible role for NrfA in NO· detoxification emerged only recently with the observation that an *E. coli nrf* strain had much greater sensitivity to NO· than the parent strain under anaerobic conditions (6, 13). The *nrf* gene products have a well established role coupling quinol oxidation to nitrite reduction during anoxic and micro-oxic growth in the presence of nitrate or nitrite (14). Quinol oxidation is catalyzed by NrfD and electrons are transferred, most likely via NrfC and NrfB, to NrfA, a homodimeric, deca-heme-containing cytochrome *c* nitrite reductase (15). NrfA homologs are present in a wide range of bacteria, and *in vitro* they have been shown to reduce not only nitrite but also NO· and hydroxylamine to ammonium without releasing detectable intermediates (15–19). As a consequence, it was proposed that NO· reduction by NrfA, rather than nonspecific reduction by another Nrf component, was responsible for providing *E. coli* with resistance toward NO· under anaerobic conditions (6).

* This work was supported by Biotechnology and Biological Sciences Research Council Grant 83/B18695 and a Joint Infrastructure Fund award for equipment (062178). The costs of publication of this article were defrayed in part by the payment of page charges. This article must therefore be hereby marked "*advertisement*" in accordance with 18 U.S.C. Section 1734 solely to indicate this fact.

[1] Present address: Laboratoire de Bioénergétique et Ingénierie des Protéines, CNRS 31, Chemin Joseph Aiguier, 13402 Marseille cedex 20, France.

[2] To whom correspondence should be addressed: School of Chemical Sciences and Pharmacy, University of East Anglia, Norwich NR4 7TJ, UK. Tel.: 44-1603-593877; Fax: 44-1603-592003; E-mail: j.butt@uea.ac.uk.

[3] The abbreviations used are: NO, nitric oxide; $i_{cat}$, catalytic current magnitude; $\Delta G^{\ddagger}$, activation free energy; $\Delta H^{\ddagger}$, activation enthalpy; $i_{max}$, maximum catalytic current magnitude; NrfA, cytochrome *c* nitrite reductase; PFV, protein film voltammetry; $\Delta S^{\ddagger}$, activation entropy; SHE, standard hydrogen electrode; Mes, 4-morpholineethanesulfonic acid; Taps, 3-{[2-hydroxy-1,1-bis(hydroxymethyl)ethyl]amino}-1-propanesulfonic acid.

*E. coli* NrfA has been reported to reduce ~450 NO· $s^{-1}$ whereas the enzyme from *Desulfovibrio desulfuricans* reduces only 30 NO· $s^{-1}$ under comparable conditions (16). In addition, it has been noted that *D. desulfuricans* NrfA exhibits similar rates of NO· and nitrite reduction whereas the enzyme from *Sulfurospirilum deleyianum* reduces NO· at one hundredth the rate of nitrite reduction (16, 17). Given these diverse observations and the proposed role for *E. coli* NrfA in NO· detoxification, we have set about providing a more complete and quantitative description of the NO· reductase activity of this enzyme. Our previous studies employed protein film voltammetry (PFV) to quantitate the nitrite and hydroxylamine reductase activities of *E. coli* NrfA (19, 21–26). In this approach graphite electrodes substituted for NrfB to deliver electrons directly to NrfA that had been adsorbed on the electrode surface. Michaelis-Menten parameters were deduced for each catalytic cycle from the variation of catalytic current (rate) with substrate concentration. In addition, enzyme activities were resolved across the electrochemical potential domain, revealing multiple modulations of the catalytic rate in response to the application of an increased driving force for the reaction being catalyzed. Because these modulations of activity were independent of the nature of the electrode surface, they were proposed to reflect intrinsic properties of NrfA nitrite and hydroxylamine reduction. Thus, to facilitate comparison with the other reductase activities of this enzyme we have chosen to define the NO· reductase activity of *E. coli* NrfA by PFV.

## EXPERIMENTAL PROCEDURES

*Protein Purification—E. coli* cytochrome *c* nitrite reductase NrfA was purified and quantitated as described previously (15). The enzyme had a specific activity of 1500 $\mu$mol nitrite consumed $min^{-1}$ $mg^{-1}$ measured by enzyme-dependent oxidation of dithionite-reduced methyl viologen (1 mM) in 1 mM nitrite, 2 mM $CaCl_2$, 50 mM Hepes, pH 7.0, at 20 °C. Samples of the enzyme in 50 mM Hepes, pH 7.0, were stored as aliquots frozen in liquid nitrogen (15).

*Reagent Preparation and NO· Quantification*—All solutions were prepared with "*Trace*-SELECT-Ultra" water (Sigma-Aldrich). The buffer-electrolyte was 2 mM $CaCl_2$, 50 mM Hepes, pH 7.4, or 25 mM each of Hepes, Mes, Taps, and acetate with 2 mM $CaCl_2$ for studies from pH 4 to 9. Stock solutions for each substrate were prepared daily. For nitrite (50 mM) the appropriate mass of $NaNO_2$ was dissolved in ice-cold buffer-electrolyte and the pH confirmed to be that desired. For hydroxylamine (2 M) the appropriate mass of $NH_2OH.HCl$ was dissolved in ice-cold buffer-electrolyte and brought to the desired pH with aliquots of 10 M NaOH.

Buffer-electrolyte solutions saturated with NO· were prepared from NO· gas (98.5%; Aldrich) that had been bubbled through an anaerobic aqueous solution of 100 mM NaOH. The NO· concentration in the resultant solution was determined by titration against a defined quantity of horse heart myoglobin. Here ferric myoglobin, $\epsilon_{410\ nm}$ = 186 $mM^{-1}$ $cm^{-1}$ (27), was reduced with sodium ascorbate and phenazine ethosulfate (final concentrations 1 mM and 5 $\mu$M, respectively) in a sealed anaerobic cuvette. Addition of aliquots of NO· caused a decrease in the peak intensity at 434 nm with concomitant appearance of a peak at 421 nm that was indicative of formation of the ferrous myoglobin-NO· complex (28). The concentrations of NO· and myoglobin in the cuvette were considered equal when NO· addition failed to perturb the spectrum. Stock solutions prepared and quantitated as described above contained between 1.7 and 2 mM NO·.

Because of the volatility of NO· its concentration in the electrochemical cell was measured immediately after each experiment. Calibration against myoglobin proved too time consuming to allow effective experimentation, so a modified version of the acidified Griess reaction was adopted to allow rapid analysis in triplicate (29). Briefly, aerobic cuvettes containing 1.9 ml of 17 mM sulfanilic acid, 0.4 mM *N*-(1-naphthyl) ethylenediamine dihydrochloride in 2 mM $CaCl_2$, 50 mM Hepes, pH 7.4, were sealed and taken into the anaerobic chamber where voltammetry was performed. Each cuvette was injected with 50 $\mu$l of the solution to be assayed, shaken for 1 min, and removed from the anaerobic chamber where 50 $\mu$l of phosphoric acid (85%) was added. The cuvettes were left for 15 min and the absorbance measured at 540 nm. NO· concentrations were calculated using $\epsilon_{540\ nm}$ = 42.2 $(mM\ NO\cdot)^{-1}$ $cm^{-1}$ determined by calibration of the modified Griess reaction with NO· solutions whose concentrations have been determined by titration against ferrous myoglobin.

*Protein Film Voltammetry*—Experiments employed a three-electrode cell configuration placed inside a Faraday cage housed in a $N_2$-filled chamber with atmospheric $O_2 < 2$ ppm as described previously (30). The jacketed sample chamber was incubated at the desired temperature by connection to a thermostatted water bath. The cell employed an Ag/AgCl (saturated KCl) reference electrode, and potentials are reported with respect to the Standard Hydrogen Electrode following addition of 197 mV to the measured potential.

Pyrolytic graphite edge working electrodes of 3-mm diameter were polished immediately prior to use with an aqueous slurry of 0.3 $\mu$m $Al_2O_3$, sonicated, rinsed, and dried with a tissue. The freshly polished electrode was then taken into the anaerobic chamber together with a frozen aliquot of NrfA (0.17 $\mu$M). Immediately the NrfA sample had thawed, 3 $\mu$l was placed on the electrode surface and after ~20 s excess solution was removed from the electrode with a tissue. The electrode was then rinsed with buffer-electrolyte and placed into the electrochemical cell. During experiments with NO· a rubber O-ring was placed around the shaft of the working electrode to form a light seal to the electrochemical cell.

To define the variation of catalytic rate with nitrite or hydroxylamine concentration, sequential additions of substrate were made to the electrochemical cell while cyclic voltammetry was performed. Each titration employed a freshly prepared NrfA film with electrode rotation at 3000 rpm where the response suffered no limitation from substrate mass transport (19, 25). To define the catalytic current due to NrfA-specific substrate reduction, the current recorded with a "bare" electrode was subtracted from that recorded with the NrfA film in place. Prior to determination of $K_m$ and $i_{max}$ the catalytic currents were adjusted for a first order loss of signal magnitude ($t_{½}$ ~ 70 min) that occurred during the course of each experiment.

For direct comparison of nitrite and NO· reduction rates a freshly prepared NrfA film was placed in nitrite and two voltammograms were measured with electrode rotation at 3000 rpm. The film was then transferred to a solution of approximately equimolar NO·. Two voltammograms were measured with electrode rotation at 100 rpm, and aliquots of the NO· solution were immediately analyzed by the Griess reaction. A rotation rate of 100 rpm gave steady state voltammetry without rapid loss of NO· from solution as occurred at higher rotation rates. Catalytic currents for nitrite reduction were calculated as above. Those for NO· reduction were obtained after subtraction of the response from a bare electrode in NO·-containing buffer-electrolyte and adjustment for a reproducible 10 (±2) % loss of magnitude due to film transfer that was identified in control experiments.

Catalytic current magnitudes were calculated at two potentials. At −0.3 V NrfA NO· reduction was detected with little or no interference from electrodic NO· reduction. At −0.4 V the current due to NrfA NO· reduction was subject to greater error due to its superposition on a contribution from electrodic NO· reduction but closer to the catalytic rate that would be achieved when the response becomes independent of further increase of driving force, *i.e.* at sufficiently negative electrode potentials. For all substrates the values of $K_m$ and maximum catalytic current magnitude ($i_{max}$) determined from Hanes and Lineweaver-Burk plots were within 15% of those determined by direct fit to the Michaelis-Menten equation. Activation enthalpies were determined from plots of ln $i_{max}$ *versus* $T^{-1}$ by fit to a modification of the Eyring equation as shown in Equation 1

$$\ln i_{max} = \ln\frac{k_b T}{h} - \frac{\Delta S^{\ddagger}}{R} - \frac{\Delta H^{\ddagger}}{RT} \qquad \text{(Eq. 1)}$$

where $\Delta S^{\ddagger}$ is the activation entropy and $\Delta H^{\ddagger}$ the activation enthalpy, $k_b$ the Boltzmann constant, $h$ the Planck constant, $R$ the gas constant, and $T$ the temperature. Fitting was performed with MicroCal Origin.

## RESULTS

*Detection of NO· Reduction by NrfA Using PFV*—Previous studies have established that electrocatalytically active NrfA films are formed when freshly polished pyrolytic graphite edge electrodes are exposed to ice-cold NrfA solutions (19, 21–23). Featureless cyclic voltammograms were observed when films of NrfA prepared in this way were placed in 2 mM $CaCl_2$, 50 mM Hepes, pH 7.4, at 4 °C with electrode rotation at 100 rpm (Fig. 1*A*, *triangles*). However, the voltammogram changed after the addition of NO·-saturated buffer-electrolyte to give 20 μM NO· in the electrochemical cell (Fig. 1*A*, *heavy solid line*). Reductive (negative) catalytic currents were detected below approximately −0.1 V. Control experiments performed with bare electrodes placed in 20 μM NO· showed evidence of catalytic reduction at potentials below approximately −0.4 V (Fig. 1*A*, *circles*). Thus, the sigmoidal catalytic response initiated just below −0.1 V can be attributed to NrfA-specific NO· reduction.

Confirmation of the voltammetric detection of NrfA NO· reduction was provided by experiments in the presence of cyanide. Cyanide is a potent inhibitor of NrfA nitrite and hydroxylamine reductase activities that is expected to inhibit NrfA-specific NO· reduction (Fig. 1*B*) (21, 22). Indeed, the sigmoidal catalytic feature just below −0.1 V arising from a NrfA film in 20 μM NO· disappeared on addition of cyanide whereas catalysis below −0.4 V, due predominantly to electrodic NO reduction, persisted with only a small drop in magnitude (Fig. 1*A*, *light solid line*).

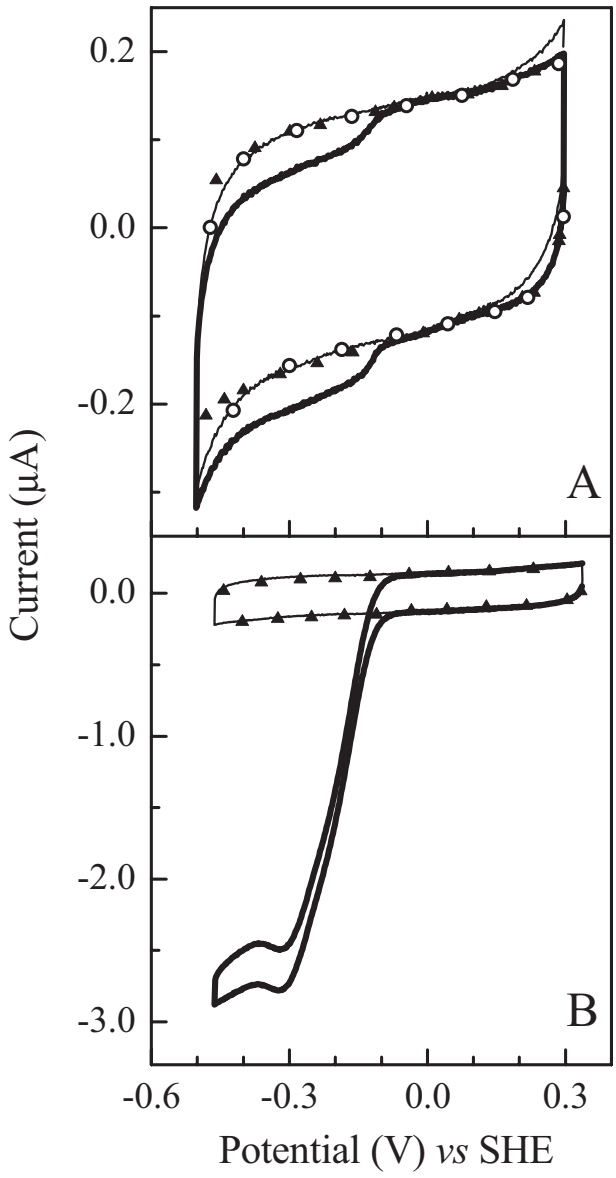


FIGURE 1. **Representative PFV of *E. coli* NrfA in NO· (*A*) and nitrite (*B*).** *A*, NrfA film in buffer-electrolyte (▲), 20 μM NO· (*heavy solid line*), and 20 μM NO· with 200 μM cyanide (*light solid line*). Bare electrode in 20 μM NO· (○). Scan rate 20 mV $s^{-1}$ with electrode rotation at 100 rpm. *B*, NrfA film in buffer-electrolyte (▲), 20 μM nitrite (*heavy solid line*), and with 20 μM nitrite and 200 μM cyanide (*light solid line*). Scan rate 20 mV $s^{-1}$ and electrode rotation at 3000 rpm. For both panels the buffer-electrolyte was 2 mM $CaCl_2$, 50 mM Hepes, pH 7.4, at 4 °C.

A comparison of the PFV from NrfA in 20 μM NO· with that in 20 μM nitrite showed reduction of both substrates occurred over a similar potential range (Fig. 1). NO· reduction was repeatedly described by much smaller catalytic currents than those due to nitrite reduction. The distinct rotation rate dependences of the catalytic responses for nitrite and NO· reduction

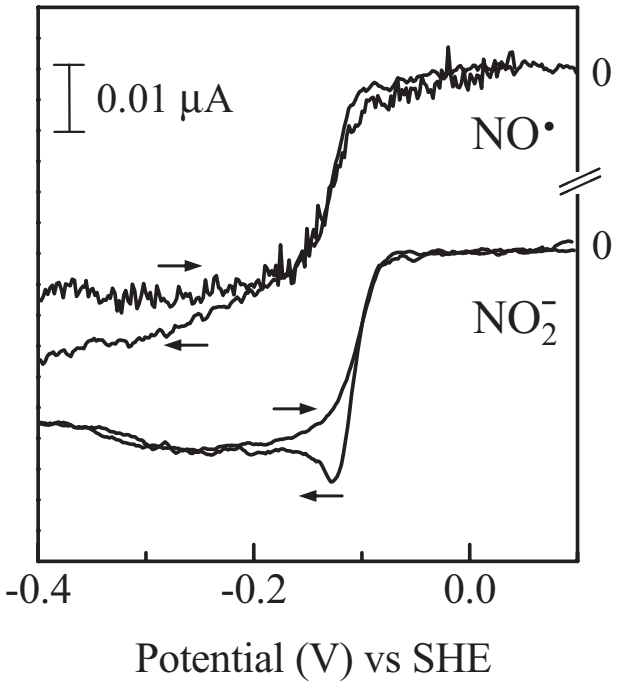


FIGURE 2. **PFV of NrfA in 20 μM NO· and 1.5 μM nitrite with electrode rotation at 100 rpm.** The voltammograms are presented after subtraction of the response from a freshly polished electrode in buffer-electrolyte. *Arrows* indicate the direction of each scan. Scan rate 20 mV $s^{-1}$ with buffer-electrolyte of 2 mM $CaCl_2$, 50 mM Hepes, pH 7.4, at 4 °C.

confirmed that trace levels of nitrite were not responsible for the catalytic response detected in the NO· experiments (Fig. 2). Voltammetry performed at 100 rpm in nitrite solutions showed a peak of current on scans to more negative potentials that was absent on the return to more positive potentials (Fig. 2). This form of response is indicative of substrate, *i.e.* nitrite, depletion in the vicinity of the adsorbed enzyme, and for this reason quantitative studies of nitrite reduction are performed at 3000 rpm where the response of the forward and reverse scans overlay (*e.g.* Fig. 1*B*) (25).

By contrast, the voltammetry in NO· solutions was essentially independent of electrode rotation rate above 90 rpm with no indication of substrate depletion at the electrode surface (Fig. 2). Below −0.2 V the catalytic current had slightly different magnitudes for the scans to positive and negative potentials but control experiments showed this arose from electrodic NO· reduction. Importantly, the response just below −0.1 V that most clearly defined NrfA NO· reduction was in good agreement for both scan directions and so indicative of a steady-state catalytic response. Having ruled out the possibility that detectable levels of nitrite were present in the NO· experiments, it was concluded that NrfA is a NO· reductase with distinct kinetic parameters for the reduction of NO· and nitrite.

*Quantitation of Steady-state NrfA Reduction of NO·, Nitrite, and Hydroxylamine*—Initial experiments to define the relationship between catalytic rate and NO· concentration involved titration of NO· into the electrochemical cell. Cyclic voltammetry showed that the catalytic rate increased as the NO· concentration increased (Fig. 3*A*). However, colorimetric quantitation of NO· at the end of the experiment showed its concentration was only 86% of that expected. Similar behavior was observed in a number of titrations, but the final NO· level ranged from 40 to 86% of that expected. Because this prevented reliable assessment of the NO· concentration at intermediate points in the titrations, an alternative experimental approach was adopted.

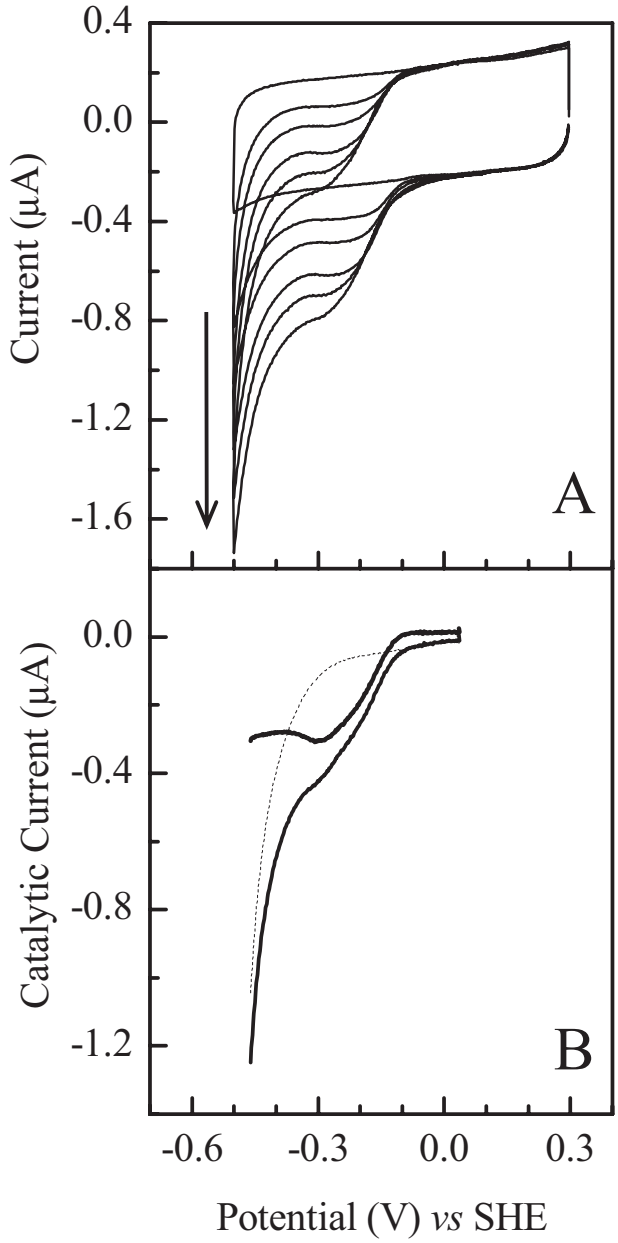


FIGURE 3. **The NO· reductase activity of NrfA.** *A*, NrfA PFV for NO· concentrations from 0 to 180 μM as indicated by the direction of the *arrow* (see "Results" for details). *B*, catalytic current from reduction of 333 μM NO· by NrfA (*heavy solid line*) obtained by subtraction of the bare electrode 333 μM NO· response (*broken line*) from NrfA PFV in 333 μM NO· (*light solid line*). Electrode rotation was at 100 rpm; all other conditions were as in Fig. 1.

After NO· addition to the cell a reproducible (3%) drop in concentration was found to have occurred after measuring two cyclic voltammograms. Thus, film transfer experiments were conducted with this restriction to assess the relative rates of nitrite and NO· reduction at a number of substrate concentrations. The relationship between nitrite concentration and reduction rate was defined under comparable conditions by a nitrite titration. The two sets of results were combined and the

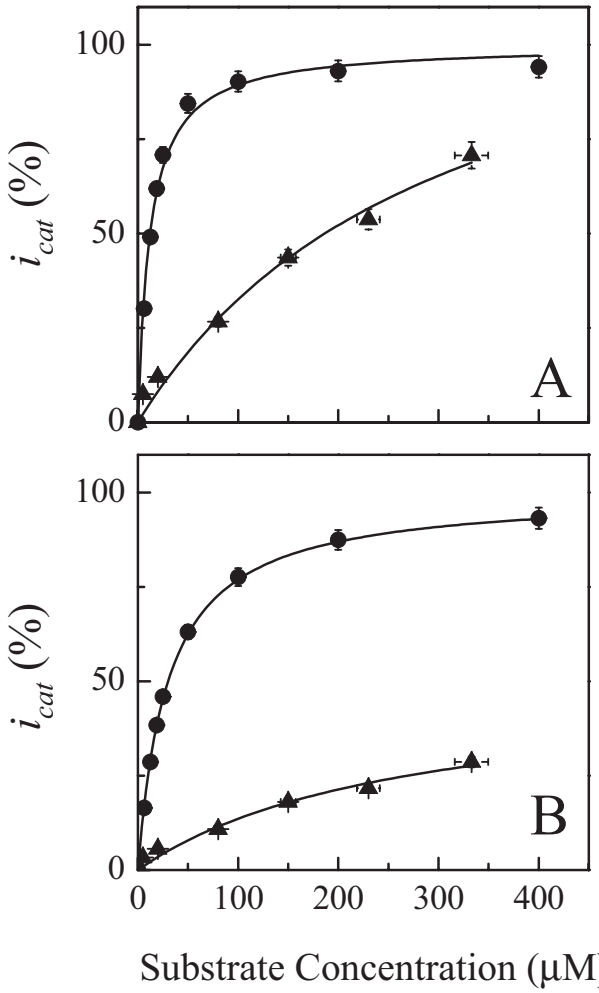


FIGURE 4. **Kinetic analysis of NrfA NO· (▲) and nitrite (●) reductase activities.** Catalytic current magnitudes ($i_{cat}$) measured at −0.3 V (*A*) and −0.4 V (*B*). The lines illustrate fits to the Michaelis-Menten equation with $K_m$ and $i_{max}$ as given in Table 1. Experimental conditions were as in Fig. 1.

resultant plots fit to the Michaelis-Menten equation (Fig. 4, Table 1. The catalytic currents recorded at −0.3 and −0.4 V showed similar trends. Maximum catalytic rates for nitrite reduction were approached above 200 μM substrate, but NO· concentrations up to 340 μM provided little indication that the maximal rate of NO· reduction was being approached. )

Here we note that two steps were taken to facilitate quantitation of the NrfA NO· response as distinct from electrodic NO· reduction. The first step was to perform experiments at 4 °C rather than 20 °C as used for previous PFV of NrfA because lower temperatures were found to improve the ratio of enzymatic to electrodic currents (not shown). The second step was to subtract the response of a freshly polished bare electrode recorded in a solution of given NO· concentration from that of the NrfA-coated electrode prior to analysis (Fig. 3*B*). Quantitative experiments were still restricted to NO· concentrations below 350 μM because the decreased ratio of enzymic to electrodic current detected at higher NO· concentrations introduced unacceptable uncertainty into quantitation of the NrfA-specific currents.

The Michaelis constants ($K_m$) and maximum catalytic currents ($i_{max}$) describing NO· and nitrite reduction are compared

**TABLE 1**

**Comparison of the kinetic parameters for NrfA reduction of nitrite, NO·, and hydroxylamine at pH 7.4 and 4 °C**

Values of $i_{max}$ are relative to that for nitrite reduction at the quoted potential. The errors are statistical from non-linear regression.

| | Analysis at −0.3 V | | Analysis at −0.4 V | |
|---|---|---|---|---|
| | $K_m$ | $i_{max}$ | $K_m$ | $i_{max}$ |
| | μM | % | μM | % |
| Nitrite | 12 ± 2 | 100 | 30 ± 4 | 100 |
| NO· | 304 ± 30 | 131 ± 10 | 283 ± 30 | 50 ± 5 |
| Hydroxylamine | 60,400 ± 4,000 | 226 ± 5 | 125,000 ± 3,000 | 268 ± 5 |

in Table 1 where, for completeness, values for hydroxylamine reduction under comparable conditions are included. The $K_m$ values increased in the order nitrite <NO· ≪hydroxylamine and differed by at least an order of magnitude. The values obtained here for nitrite and hydroxylamine reduction are comparable with those of ~25 and 127,000 μM, respectively, at 20 °C, pH 7.0, (19). We considered that the fits to the NO· data might be less reliable because the experimentally attained rates approached only 50% of $i_{max}$ whereas those for nitrite and hydroxylamine reduction approached 90% of their respective maxima. Analysis of the nitrite reduction data for rates less than 50% of $i_{max}$ yielded $K_m$ values twice as large and $i_{max}$ values within 30% of those from the full data set. However, the kinetic parameters for NrfA substrate reduction are such that this possible error does not alter the major conclusions drawn from Table 1, namely that at 4 °C and pH 7 all three substrates are reduced with similar maximal velocities but with significantly different $K_m$values. The higher $K_m$ for NO· than nitrite reduction was confirmed experimentally when it was found that the mass transport limited response from reduction of 2 μM nitrite observed at 100 rpm was only lost on addition of ~10-fold more NO· to the solution.

Catalytic waves for NrfA reduction of NO·, nitrite, and hydroxylamine are compared in Fig. 5. To facilitate their comparison these waves are presented at substrate concentrations corresponding to ~100, 75, 25, and 5% of their respective $K_m$ values at −0.4 V because this encompassed the range of NO· concentrations from which data could be confidently extracted. At these concentrations the activity of NrfA toward all three substrates is initiated just below −0.1 V but the wave shapes are clearly substrate-dependent. Hydroxylamine reduction gives rise to essentially sigmoidal responses whereas the NO· reduction waves show a peak of activity. By contrast, the nitrite reduction waves changed from peak-shaped to reflect a low potential activity "boost" as the nitrite concentration increased.

*pH and Temperature Dependence of NrfA NO· Reduction Rates*—To assess the pH dependence of NrfA NO· reductase activity, films were transferred between solutions of distinct pH, each containing 50 μM NO· (Fig. 6). Exposure to more acidic pH results in a sigmoidal increase of activity that is accompanied by displacement of the catalytic wave toward more positive potentials. These changes were independent of the order of exposure to pH and so fully reversible.

Film transfer experiments with each substrate at a concentration equal to its $K_m$ at 4 °C demonstrated that NrfA activity toward all three substrates increased when the temperature was raised from 4 to 25 °C. The rates increased linearly with tem-

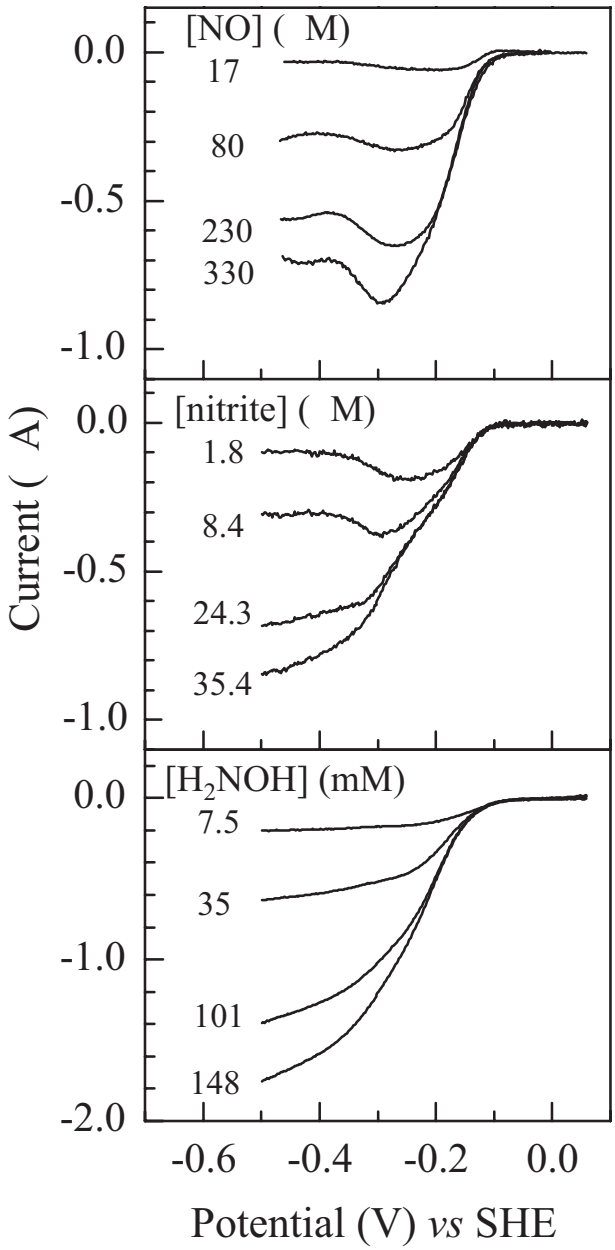


FIGURE 5. **Representative catalytic current potential profiles from films of *E. coli* NrfA in NO·, nitrite, and hydroxylamine.** The substrate concentrations correspond to ~100, 75, 50, and 5% of their respective $K_m$ values. Voltammetry was at 20 mV $s^{-1}$ with electrode rotation at 100 rpm for NO· and 3000 rpm for nitrite and hydroxylamine. Other conditions were as in Fig. 1.

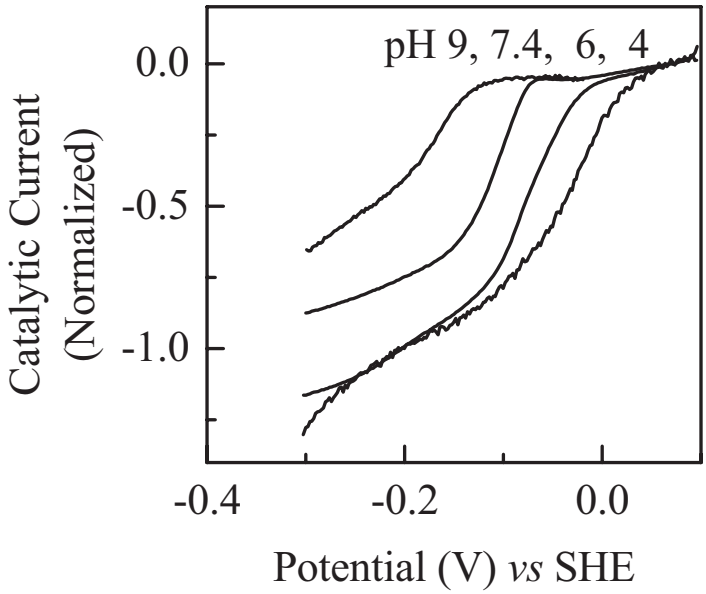


FIGURE 6. **pH dependence of NrfA PFV in 50 $\mu$M NO·.** The response of a bare electrode in buffer-electrolyte was subtracted from the PFV to give the catalytic current. Scan rate 20 mV $s^{-1}$, electrode rotation rate 100 rpm, and buffer-electrolyte 2 mM $CaCl_2$, 25 mM Hepes, 25 mM Mes, 25 mM Taps, 25 mM acetate at the pH values indicated, 4 °C.

**TABLE 2**
**Ratio of the catalytic current at 25 °C to that at 4 °C**
Substrate concentration = $K_m$, pH 7.4.

| | Nitrite | NO· | Hydroxylamine |
|---|---|---|---|
| −0.3 V | 2.7 ± 0.2 | 2.5 ± 0.3 | 6.2 ± 0.2 |
| −0.4 V | 2.2 ± 0.2 | 2.5 ± 0.3 | 8.0 ± 0.2 |

perature, and the increase was significantly greater for reduction of hydroxylamine than for nitrite and NO· (Table 2). With the assumption that the $K_m$ for NO· reduction, like those for nitrite and hydroxylamine reduction, is independent of temperature across this range, the variations in rates reflect the variation of $i_{max}$ with temperature. Fits of the data to the Eyring equation provided activation enthalpies ($\Delta H^{\ddagger}$) of ~25 kJ $mol^{-1}$ for nitrite and NO· reduction and ~65 kJ $mol^{-1}$ for hydroxylamine reduction.

## DISCUSSION

The work presented here has shown that *E. coli* NrfA is able to serve as a direct NO· reductase. This demonstration can explain the increased sensitivity of anaerobically grown *E. coli nrf* mutants to NO· when compared with the parent strain in addition to the strongly attenuated ability of the mutants to remove NO· from anoxic cultures (6, 13). Similar maximum catalytic rates are predicted for NO· and nitrite reduction. Because we do not know the amount of electrocatalytically active enzyme adsorbed on the electrode surface, we cannot directly convert maximum catalytic current to a turnover number ($k_{cat}$). However, in solution assays at room temperature with reduced methyl viologen as the electron donor, NrfA nitrite reduction occurs with a $k_{cat}$ of ~700 $NO_2^-$ $s^{-1}$ that corresponds to an electron flux of ~4200 $s^{-1}$ (13, 15). If the enzyme, as the PFV suggests, can reach similar electron flux during NO· reduction this corresponds to a $k_{cat}$ of ~840 $s^{-1}$. This is a value much higher than those so far reported for flavohemoglobin and flavorubredoxin from *E. coli* and the dedicated respiratory NO· reductases of *P. denitrificans* and *Ps. stutzeri* (4, 5, 7–12).

During colonization of a human host, *E. coli* will experience predominantly micro-oxic and anoxic environments along with concentrations of nitrate and nitrite that should result in production of NrfA and flavorubredoxin, both of which may play a role in NO· detoxification (11, 31, 32). At pH 7, the $K_m$ of ~300 $\mu$M for NO· removal by NrfA is clearly much larger than that of 0.4 $\mu$M displayed by flavorubredoxin (11, 12). However, the much higher turnover number predicted for NrfA results in a specificity constant ($k_{cat}/K_m$) of ~$2 \times 10^6$ $M^{-1}$ $s^{-1}$ that lies

within an order of magnitude of that of $\sim 40 \times 10^6\ M^{-1}\ s^{-1}$ for the cytoplasmically located flavorubredoxin. We estimate that NrfA will reduce 27 NO· $s^{-1}$ at the 10 $\mu$M NO· levels produced extracellularly by activated macrophages (33). Thus, in considering the manner by which *E. coli* detoxifies exogenous NO· encountered during invasion of a human host it may be that NrfA maintains low NO· levels in the periplasm so that any NO· that does reach the cytoplasm is efficiently removed by flavorubredoxin.

The ability of NrfA to reduce NO· in addition to nitrite offers *E. coli* the opportunity for respiratory flexibility and NO detoxification in a single enzyme. The 10-fold greater $K_m$ for NrfA reduction of NO· than nitrite implies that the NO· reductase activity will come into its own when NO· concentrations are elevated significantly above those of nitrite. Given that activated macrophages can produce extracellular NO· concentrations on the order of 10 $\mu$M, such elevated NO· levels may be encountered when *E. coli* is phagocytosed by resident macrophages (33). Conditions that could favor NrfA NO· reduction may also arise in the rapidly changing environments of the gastrointestinal tract and are perhaps most likely in the acidic conditions of the stomach where nitrite disproportionates to a range of species, including NO· (3). As a periplasmic protein NrfA will be subject to the wide range of pH exploited by the gastrointestinal tract (34), and our demonstration that NrfA NO· reductase activity persists over a pH range of at least six units from pH 3 to 9 is consistent with retention of NrfA activity on passage through the gastrointestinal tract.

There is little information available on the levels of hydroxylamine that may be encountered by *E. coli* and that could allow the hydroxylamine reductase activity of NrfA to placed in a physiological context (35). However, comparison of NrfA activity toward hydroxylamine in addition to NO· and nitrite is valuable when considering the biochemical implications of our results. Each NrfA subunit contains five *c*-type hemes. Four of these hemes have *bis*-histidine ligation and the fifth has lysine and water (hydroxide) as axial ligands (15). Crystal structures of *Wolinella succinogenes* NrfA complexed with nitrite and hydroxylamine show that these substrates displace water (hydroxide) to become axial ligands to the lysine-coordinated heme and in so doing they define the site for binding and reduction of these substrates (20). Here we make several observations that point toward the site of NO· reduction overlapping with that for nitrite and hydroxylamine reduction. Specifically, nitrite competes with NO· for reduction by NrfA, reduction of all three NrfA substrates is strongly inhibited by cyanide (21, 22), and reduction of all three substrates is initiated at similar potentials that we have proposed to reflect in part the reduction potential of the lysine-coordinated heme (19). In addition, the nitrite and NO· reductase activities of NrfA show similar variation in rate and operating potentials with pH, suggesting that the same ionizable group(s) may modulate both activities. Thus, we propose that the lysine-coordinated heme forms the site of NO· binding and reduction in NrfA.

The detailed mechanism(s) of NrfA substrate reduction have yet to be conclusively demonstrated. Nitrite, NO·, and hydroxylamine are each reduced stoichiometrically to ammonium such that no intermediates are detectable (15–19). Because all three substrates form the same product it has been suggested that NO· and hydroxylamine are intermediates during nitrite reduction. A computational study and comparison to the chemistry of model complexes have supported this proposal, and in this context some discussion of the information from this study is warranted (20). The relative order of the $K_m$ values, with that for nitrite < NO· ≪ hydroxylamine, is not immediately reconciled with the failure to detect reaction intermediates. The active site is buried deep in the interior of the enzyme with two channels providing access to the exterior (15). One channel is positively charged whereas the other is negatively charged, making it an attractive proposition that the first channel allows nitrite to access the active site while the second is for ammonium egress. We cannot know through which channel NO·, or indeed hydroxylamine, enter the active site, but in either case the channel is unlikely to have a high affinity for substrate and this may then be reflected in the measured $K_m$.

NrfA also reduces these three substrates at distinct rates. The maximum rate of hydroxylamine reduction is greater than those for NO· and nitrite reduction at physiological temperatures with the rate-limiting step lying between NO· and hydroxylamine. The variation of predicted maximal catalytic rates with temperature yields a higher activation enthalpy for hydroxylamine reduction than those for reduction of NO· and nitrite. Higher catalytic rates must reflect a smaller activation free energy and so the activation entropy for hydroxylamine reduction must be larger than those for NO· and nitrite. Differences in NrfA processing of the substrates are also manifest in the catalytic wave shapes observed at lower substrate concentrations. The peaked responses, more prominent for nitrite reduction at higher temperatures than the 4 °C used in this study, were previously proposed to arise from activation of the enzyme on reduction of active site heme followed by attenuation of activity on reaching potentials low enough to reduce one or more of the *bis*-histidine-coordinated hemes lying near the dimer interface (19). The mechanism by which heme reduction attenuates activity is not clear. Because the phenomenon is not apparent during hydroxylamine reduction, one possibility was that it reflected a change in coordination capabilities within the active site that had a greater effect for nitrite, with two N–O bonds, than hydroxylamine. However, it now appears that it is unlikely because NO· reduction gives rise to peaked wave shapes. Alternative mechanisms for modulation of catalytic rate include redox-linked modulations of intra-molecular electron and proton transfer.

*Acknowledgments—We thank Christine Moore for purifying NrfA and Jeff Cole, Andrew Hemmings, and Tom Clarke for helpful discussions.*

## REFERENCES

1. Snyder, S. H., and Bredt, D. S. (1992) *Sci. Am.* **266,** 68
2. Alderton, W. K., Cooper, C. E., and Knowles, R. G. (2001) *Biochem. J.* **357,** 593–615
3. Benjamin, N., Odriscoll, F., Dougall, H., Duncan, C., Smith, L., Golden, M., and McKenzie, H. (1994) *Nature* **368,** 502–502
4. Heiss, B., Frunzke, K., and Zumft, W. G. (1989) *J. Bacteriol.* **171,** 3288–3297

5. Fujiwara, T., and Fukumori, Y. (1996) *J. Bacteriol.* **178,** 1866–1871
6. Poock, S. R., Leach, E. R., Moir, J. W. B., Cole, J. A., and Richardson, D. J. (2002) *J. Biol. Chem.* **277,** 23664–23669
7. Poole, R. K. (2005) *Biochem. Soc. Trans.* **33,** 176–180
8. Justino, M. C., Vicente, J. B., Teixeira, M., and Saraiva, L. M. (2005) *J. Biol. Chem.* **280,** 2636–2643
9. Poole, R. K., and Hughes, M. N. (2000) *Mol. Microbiol.* **36,** 775–783
10. Gardner, P. R. (2005) *J. Inorg. Biochem.* **99,** 247–266
11. Gardner, A. M., Helmick, R. A., and Gardner, P. R. (2002) *J. Biol. Chem.* **277,** 8172–8177
12. Gomes, C. M., Giuffre, A., Forte, E., Vicente, J. B., Saraiva, L. M., Brunori, M., and Teixeira, M. (2002) *J. Biol. Chem.* **277,** 25273–25276
13. Clarke, T. A., Mills, P. C., Poock, S. R., Butt, J. N., Cheesman, M. R., Cole, J. A., Hinton, J. D., Hemmings, A. M., Kemp, G., Soderberg, C. A. G., Spiro, S., van Wonderen, J., and Richardson, D. J. (2008) *Methods Enzymol.* in press
14. Simon, J. (2002) *FEMS Microbiol. Rev.* **26,** 285–309
15. Bamford, V. A., Angove, H. C., Seward, H. E., Thomson, A. J., Cole, J. A., Butt, J. N., Hemmings, A. M., and Richardson, D. J. (2002) *Biochemistry* **41,** 2921–2931
16. Costa, C., Macedo, A., Moura, I., Moura, J. J. G., Legall, J., Berlier, Y., Liu, M. Y., and Payne, W. J. (1990) *FEBS Letts.* **276,** 67–70
17. Stach, P., Einsle, O., Schumacher, W., Kurun, E., and Kroneck, P. M. H. (2000) *J. Inorg. Biochem.* **79,** 381–385
18. Kajie, S. I., and Anraku, Y. (1986) *Eur. J. Biochem.* **154,** 457–463
19. Angove, H. C., Cole, J. A., Richardson, D. J., and Butt, J. N. (2002) *J. Biol. Chem.* **277,** 23374–23381
20. Einsle, O., Messerschmidt, A., Huber, R., Kroneck, P. M. H., and Neese, F. (2002) *J. Am. Chem. Soc.* **124,** 11737–11745
21. Gwyer, J. D., Richardson, D. J., and Butt, J. N. (2004) *Biochemistry* **43,** 15086–15094
22. Gwyer, J. D., Angove, H. C., Richardson, D. J., and Butt, J. N. (2004) *Bioelectrochemistry* **63,** 43–47
23. Gwyer, J. D., Richardson, D. J., and Butt, J. N. (2006) *Biochem. Soc. Trans.* **34,** 133–135
24. Burlat, B., Gwyer, J. D., Poock, S., Clarke, T., Cole, J. A., Hemmings, A. M., Cheesman, M. R., Butt, J. N., and Richardson, D. J. (2005) *Biochem. Soc. Trans.* **33,** 137–140
25. Gwyer, J. D., Richardson, D. J., and Butt, J. N. (2005) *J. Am. Chem. Soc.* **127,** 14964–14965
26. Gwyer, J. D., Zhang, J. D., Butt, J. N., and Ulstrupy, J. (2006) *Biophys. J.* **91,** 3897–3906
27. Seward, H. E. (1999) *Magneto-optical Spectroscopy of Hemoproteins* Ph.D. thesis, University of East Anglia, Norwich, UK
28. Millar, S. J., Moss, B. W., and Stevenson, M. H. (1996) *Meat Sci.* **42,** 277–288
29. Ridnour, L. A., Sim, J. E., Hayward, M. A., Wink, D. A., Martin, S. M., Buettner, G. R., and Spitz, D. R. (2000) *Anal. Biochem.* **281,** 223–229
30. Anderson, L. J., Richardson, D. J., and Butt, J. N. (2001) *Biochemistry* **40,** 11294–11307
31. Kelm, M. (1999) *Biochim. Biophys. Acta* **1411,** 273–289
32. da Costa, P. N., Teixeira, M., and Saraiva, L. M. (2003) *FEMS Microbiol. Lett.* **218,** 385–393
33. Raines, K. W., Kang, T. J., Hibbs, S., Cao, G.-L., Weaver, J., Tsai, P., Baillie, L., Cross, A. S., and Rosen, G. M. (2006) *Infect. Immun.* **74,** 2268–2276
34. Wilks, J. C., and Slonczewski, J. L. (2007) *J. Bacteriol.* **189,** 5601–5607
35. Donzelli, S., Switzer, C. H., Thomas, D. G., Ridnour, L. A., Espey, G., Isenberg, J. S., Tocchetti, C. G., King, S. B., Lazzarino, G., Miranda, K. M., Roberts, D. D., Feelisch, M., and Wink, D. A. (2006) *Antiox. Redox Signal.* **8,** 1363–1371